



Structure-directed expansion of biphenyl-pyridone derivatives as potent non-nucleoside reverse transcriptase inhibitors with significantly improved potency and safety[☆]

Li-Min Zhao^{a,b,c}, Christophe Pannecouque^d, Erik De Clercq^d, Shuai Wang^{a,b,*}, Fen-Er Chen^{a,b,c,*}

^a Engineering Center of Catalysis and Synthesis for Chiral Molecules, Department of Chemistry, Fudan University, Shanghai 200433, China

^b Shanghai Engineering Center of Industrial Asymmetric Catalysis for Chiral Drugs, Shanghai 200433, China

^c Key Laboratory of Natural Resources of Changbai Mountain & Functional Molecules, Ministry of Education, Yanbian University College of Pharmacy, Yanbian University, Yanji 133002, China

^d Rega Institute for Medical Research, KU Leuven, Herestraat 49, Leuven B-3000, Belgium

ARTICLE INFO

Article history:

Received 10 January 2023

Revised 16 February 2023

Accepted 21 February 2023

Available online 1 March 2023

Keywords:

HIV-1

NNRTI

Doravirine

Biphenyl-pyridone

Safety

ABSTRACT

Following our previous work on human immunodeficiency virus-1 (HIV-1) non-nucleoside reverse transcriptase inhibitors (NNRTIs), a series of novel biphenyl-pyridone derivatives were synthesized and evaluated for their anti-HIV-1 activity to expand their structure-activity relationship. Some of them exhibited low nanomolar activity toward wild-type HIV-1 and clinically relevant single/double mutant strains. The most active compound **B1** was 231-fold more potent ($EC_{50} = 17 \text{ nmol/L}$) than the lead compound **2** ($EC_{50} = 3.93 \text{ } \mu\text{mol/L}$) against wild-type (WT) HIV-1. This compound was approximately 3.5-fold less cytotoxic ($CC_{50} = 100.58 \text{ } \mu\text{mol/L}$) than compound **2** ($CC_{50} = 28.24 \text{ } \mu\text{mol/L}$), presenting a higher selectivity index (SI) value of 5923. Compared with **2**, the antiviral potency of **B1** was significantly increased against five single mutant strains (L100I, K103N, E138K, Y181C and Y188L) and two double mutant strains (F227L+V106A and K103N+Y181C). Especially, K103N, Y181C and K103N+Y181C were more sensitive to **B1** than both **2** and doravirine. Besides, the enzymatic inhibitory activity of **B1** against wild-type HIV-1 reverse transcriptase was approximately 32-fold higher ($IC_{50} = 100 \text{ nmol/L}$) than **2** ($IC_{50} = 3.21 \text{ } \mu\text{mol/L}$). Molecular docking studies and dynamic simulations were conducted to explain their potent activity. Taken together, this research represents an important step toward the discovery of novel biphenyl-pyridone drug candidates for HIV therapy.

© 2023 Published by Elsevier B.V. on behalf of Chinese Chemical Society and Institute of Materia Medica, Chinese Academy of Medical Sciences.

Acquired immunodeficiency syndrome (AIDS), caused by human immunodeficiency virus (HIV) infection, is currently one of the major pandemics [1,2]. In 2021, more than 38.4 million people living with HIV have been reported globally, along with about 650,000 deaths [3]. Targeting reverse transcriptase has proven to be an effective strategy for HIV treatment [4–8]. Non-nucleoside reverse transcriptase inhibitors (NNRTIs), a key component of active antiretroviral therapy (ART), effectively inhibit reverse transcriptase by targeting its allosteric binding site, which was located approximately 10 Å from the catalytic site of DNA polymerase [9–12]. Although the six Food and Drug Administration (FDA)-

approved NNRTIs, such as etravirine (ETR) and doravirine (DOR), have achieved significant clinical efficacy in the treatment of HIV, the rapid emergence of drug resistance remains a critical issue, leading to treatment failure [13,14]. Therefore, continued efforts to develop novel NNRTIs with good drug resistance and low toxicity are still urgently needed.

Recently, the displacement of 5-chloro-3-cyanophenyl of DOR with a larger biphenyl ring was first proposed by us to strengthen π - π stacking and hydrophobic interactions with surrounding aromatic hydrophobic residues Y188, Y181, F227 and W229, affording a series of biphenyl-pyridone derivatives [15]. Notably, transfer of the methyl group from 4-position of the biphenyl ring to 2-position resulted in a 2-fold increase in potency against wild-type (WT) HIV-1 with the 50% effective concentration (EC_{50}) value of 3.93 $\mu\text{mol/L}$ and slightly reduced cytotoxicity [the 50% cytotoxic concentration (CC_{50}) = 33.82 $\mu\text{mol/L}$], as shown in Fig. S1 (Support-

[☆] Dedication to Prof. Lixin Dai on the Occasion of His Centenary Birthday.

* Corresponding authors.

E-mail addresses: rfchen@fudan.edu.cn (F.-E. Chen), shuaiwang@fudan.edu.cn (S. Wang).

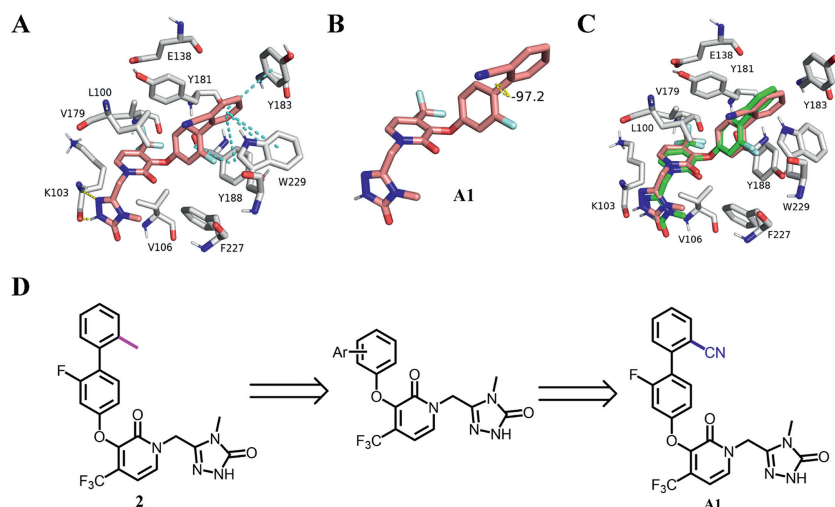


Fig. 1. (A, B) Rendering of computed structure for **A1** (pink) with wide type HIV-1 reverse transcriptase (PDB code: 4NCG); (C) Overlay of **A1** and **2** within the binding pocket; (D) Structure-directed optimization for the parent biphenyl-pyridone **2**.

ing information). The main difference in the docking results was that the biphenyl ring of compound **1** formed three π - π stacking interactions with W299 and Y181, while the biphenyl fragment of compound **2** not only maintained the same interactions with W299 and Y181 but also interacted with Y188 and Y183 via a π - π stacking interaction, respectively. The transfer of the methyl group from the 4-position to the 2-position enlarged the dihedral angle of the biphenyl ring, and oriented the molecule more favorably, thereby contributing to increasing the binding affinity between the target molecule **2** and the protein.

As part of our ongoing research on NNRTIs [16–21], we initiated this project to search for biphenyl-pyridone anti-HIV drug candidates with good drug-like properties. *Ortho*-substitution of different structural groups on the biphenyl ring was preserved in the following structural optimization, which may have potential conformational implications for enhanced potency. The molecular toxicity prediction using discovery studio suggested that the replacement of the *ortho*-methyl group of **2** with a CN group would boost its security (Table S1 in Supporting information). Molecular docking studies showed that the designed compound **A1** was well projected into the binding pocket of WT HIV-1 reverse transcriptase (Fig. 1A). In addition to maintaining three π - π stacking interactions with W299 and Y183, compound **A1** formed two π - π stacking interactions with Y188, which was different from **2**, and its dihedral angle of the biphenyl ring was further enlarged (Fig. 1B). No other differences were observed in the superposition of **A1** and **2** (Fig. 1C). Based on the above hypothesis, a series of novel biphenyl-pyridone derivatives were synthesized, and their anti-HIV-1 activity and cytotoxicity were evaluated.

The synthetic route of the target compounds **A1**–**A17** was depicted in Scheme 1A [15]. The nucleophilic substitution of the commercially available chloropyridine and appropriate *p*-bromophenols (**3a**–**3h**) was conducted using K_2CO_3 as base in NMP at 80 °C for 5 h, producing phenylchloropyridines **4a**–**4h** in 30%–92% yields. Hydrolysis of the chloropyridine with NaOH resulted in hydroxypyridines **5a**–**5h** in 66%–81% yields, followed by being treated with 5-(chloromethyl)-4-methyl-2,4-dihydro-3H-1,2,4-triazol-3-one in dry DMF to give key bromopyridine intermediates **6a**–**6h** in 66%–85% yields. Finally, **6a**–**6h** were then subjected to Suzuki coupling reaction, catalyzed by Pd(dppf)Cl₂ at 110 °C, delivering the desired products **A1**–**A17** in 60%–78% yields [22]. Schemes 1B and C described the same synthetic approach of target compounds **B1**–**B3** and **C1**–**C11** as **A1**–**A17**.

Table 1

Activity and cytotoxicity of compounds **A1**–**A17** against HIV-1 (IIIB) strains in MT-4 cells.

Compd.	R ¹	R ²	EC ₅₀ (μmol/L) ^a	CC ₅₀ (μmol/L) ^b	SI ^c
A1	2-F	CN	0.36 ± 0.06	121.58 ± 21.11	334.17
A2	2-F	F	7.77 ± 4.81	109.45 ± 34.81	14.08
A3	H	CN	4.44 ± 0.47	146.91 ± 5.61	33.12
A4	H	F	23.95 ± 6.68	129.26 ± 31.32	5.4
A5	H	CH ₃	7.68 ± 0.78	50.95 ± 2.95	6.63
A6	2-Cl	CH ₃	3.39 ± 0.32	24.81 ± 7.11	7.33
A7	2-CH ₃	CN	1.07 ± 0.24	107.5 ± 34.42	100.52
A8	2-CH ₃	F	30.78 ± 0	71.96 ± 24.52	2.34
A9	2-CH ₃	CH ₃	2.75 ± 0.67	99.96 ± 94.43	36.30
A10	3-F	CN	2.71 ± 0.68	109.78 ± 34.07	40.44
A11	3-F	F	18.43 ± 9.2	104.19 ± 42.24	5.65
A12	3-F	CH ₃	8.66 ± 1.43	27.56 ± 3.32	3.18
A13	3-Cl	CH ₃	5.78 ± 1.77	26.89 ± 5.40	4.66
A14	3-CH ₃	CN	2.18 ± 0.74	110.91 ± 39.97	50.93
A15	3-CH ₃	F	9.35 ± 4.77	101.5 ± 40.59	10.85
A16	3-CH ₃	CH ₃	4.97 ± 1.51	44.45 ± 19.27	8.94
A17	3,5-2F	CH ₃	3.37 ± 0.44	24.62 ± 3.06	7.30
2	2-F	CH ₃	3.93 ± 0.39	33.82 ± 2.52	8.60
DOR	—	—	0.013 ± 0.004	293.24 ± 0.17	22,556.92

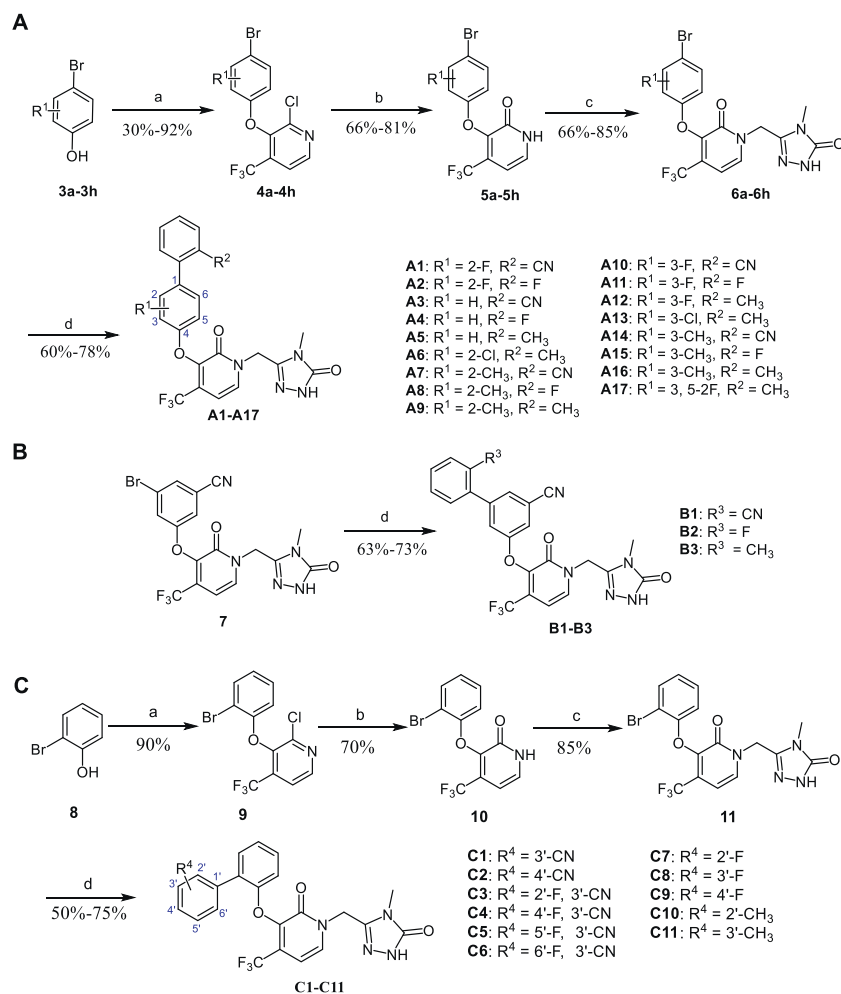
^a EC₅₀: Concentration of compound required to achieve 50% protection of MT-4 cell cultures against HIV-1-induced cytotoxicity, as determined by the MTT method, and values are the mean ± standard deviation (SD) of at least two parallel tests.

^b CC₅₀: Concentration required to reduce the viability of mock-infected cell cultures by 50%, as determined by the MTT method, and values were averaged from at least four independent experiments.

^c SI: Selectivity index, the ratio of CC₅₀/EC₅₀.

All the newly synthesized compounds were evaluated for their antiviral activity and cytotoxicity in MT-4 cells infected with WT HIV-1 strain (IIIB), with DOR as the reference drug. The biological results were summarized in Tables 1 and 2 and expressed as EC₅₀ (anti-HIV potency), CC₅₀ (cytotoxicity), and selectivity index (SI, CC₅₀/EC₅₀ ratio).

As shown in Table 1, the replacement of the *ortho*-methyl group of **2** with a CN group led to significant increase in potency toward WT HIV-1 (**A1**, EC₅₀ = 0.36 μmol/L) and much lower cytotoxicity (CC₅₀ = 121.58 μmol/L), which was consistent with our predicted results. Subsequently, the substitution of the *ortho*-methyl group with a fluorine substituent resulted in decreased activity (**A2**, EC₅₀ = 7.77 μmol/L). When the 2-F substituent of **A1** and **A2** was removed, the activity of compounds **A3** and **A4** was significantly reduced, which was similar to the trend of compound **2** in deleting the 2-F substituent. Comparable activity was obtained



Scheme 1. Synthesis of compounds **A1–A17** (A), **B1–B3** (B) and **C1–C11** (C). Reagents and conditions: (a) 2-chloro-3-fluoro-4-(trifluoromethyl)pyridine, K₂CO₃, NMP, 80 °C, 5 h; (b) NaOH, *t*-BuOH, 70 °C; (c) 5-(chloromethyl)-4-methyl-2,4-dihydro-3H-1,2,4-triazol-3-one, K₂CO₃, dry DMF, –10 °C, 30 min; (d) ArB(OH)₂, Pd(dppf)Cl₂, K₂CO₃, Dioxane, H₂O, 120 °C, 12 h.

Table 2
Activity and cytotoxicity of compounds **B1–B3** and **C1–C11** against HIV-1 (IIIB) strains in MT-4 cells.

Compd.	R ³ or R ⁴	EC ₅₀ (μmol/L)	CC ₅₀ (μmol/L)	SI
B1	CN	0.017 ± 0.008	100.58 ± 23.88	5922.94
B2	F	0.018 ± 0.006	56.17 ± 1.75	3111.63
B3	CH ₃	0.033 ± 0.004	23.47 ± 7.12	714.19
C1	3'-CN	0.74 ± 0.37	7.95 ± 2.67	10.74
C2	4'-CN	0.77 ± 0.28	27.6 ± 3.88	35.98
C3	2'-F,3'-CN	3.8 ± 2.04	17.05 ± 3.02	4.48
C4	4'-F,3'-CN	0.57 ± 0.18	11.25 ± 4.09	19.66
C5	5'-F,3'-CN	0.3 ± 0.07	42.2 ± 4.04	139.47
C6	6'-F,3'-CN	3.06 ± 0.77	78.84 ± 20.62	25.80
C7	2'-F	9.1 ± 2.89	>271.67	>30
C8	3'-F	2.74 ± 0.65	37.11 ± 3.17	15.53
C9	4'-F	3.9 ± 1.09	44.36 ± 4.55	11.37
C10	2'-CH ₃	8.43 ± 0.04	>274	>33
C11	3'-CH ₃	9.38 ± 1.85	43.02 ± 3.39	4.58
DOR	–	0.013 ± 0.004	293.24 ± 0.17	22,556.92

by replacing the 2-F substituent of **2** with a chlorine substituent or a methyl group (**A6** and **A9**). Introducing a methyl group to replace the fluorine substituent of **A1** or **A2** decreased their potency (**A7** and **A8**). The incorporation of a fluorine substituent or a methyl group at the 3-position of **A3–A5** did not improve their potency. Shifting the methyl group of **A6** from the 2-position to the 3-position resulted in reduced activity (**A13**). Introducing a fluorine

substituent to the 5-position of the biphenyl ring of **A12** doubled its potency (**A17**, EC₅₀ = 3.37 μmol/L), but did not alter cytotoxicity. Pleasingly, when the *para*-biphenyl group of **A3–A5** was changed to the *meta*-biphenyl group, the potency of **B1–B3** was significantly improved with nanomolar activity toward WT HIV-1 (IIIB) strain, as shown in Table 2. Especially, the most active compound **B1** bearing an *ortho*-CN group possessed comparable activity to DOR with an EC₅₀ value of 17 nmol/L, about 231-fold more potent than **2** (EC₅₀ = 3.93 μmol/L). The cytotoxicity of **B1** was three times lower (CC₅₀ = 100.58 μmol/L) than **2** (CC₅₀ = 28.24 μmol/L). In addition, compounds **A1–A17** and **B1–B3** displayed no inhibitory activity against HIV-2 strain (ROD) with EC₅₀ values over 35 μmol/L.

Next, we further surveyed the effect of *ortho*-biphenyl group on activity and the results were collected in Table 2. Some of them, including **C1**, **C2**, **C4** and **C5**, showed nanomolar inhibitory activity against WT HIV-1, but not as potently as **B1**. Moreover, most of them possessed unsatisfactory cytotoxicity and selectivity. The structure-activity relationship was as follows: **C1** and **C2** with a 3'-CN or 4'-CN group had similar inhibitory activity toward WT HIV-1, better than **2**. The incorporation of fluorine atom at the 2' and 6' positions of **C1** decreased its potency, but its activity slightly increased when fluorine atom was installed at the 4' and 5' positions of **C1**. Compared with **2**, no obvious potency change was observed in compounds **C7–C9** with a fluorine atom at the 2', 3', or 4' position of the biphenyl ring. Replacing the fluorine atom

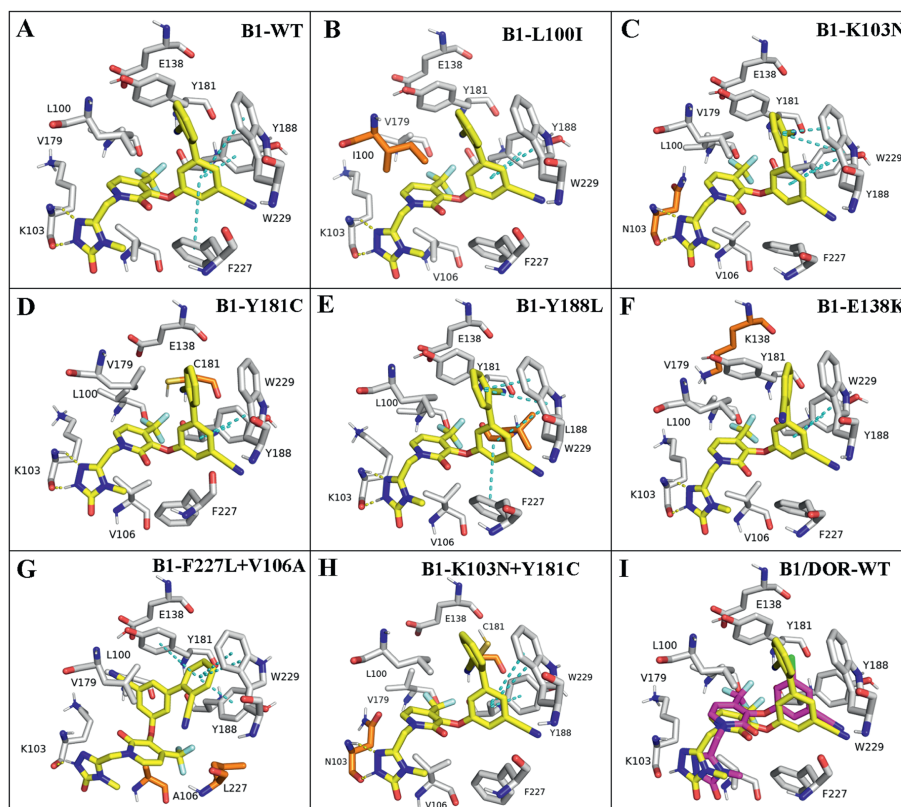


Fig. 2. Predicted binding modes of **B1** (yellow) with HIV-1 RT and mutants (PDB code: 4NCG). (A) WT with **B1**; (B) L100I with **B1**; (C) K103N with **B1**; (D) Y181C with **B1**; (E) Y188L with **B1**; (F) E138K with **B1**; (G) F227L+V106A with **B1**; (H) K103N+Y181C with **B1**; and (I) WT with **B1** (yellow) and DOR (pink). Mutated residues are depicted as orange sticks. Hydrogen bonds are depicted as yellow dashed lines and π - π bonds are shown as blue dashed lines.

Table 3

Inhibitory activity of selected compounds toward clinically relevant HIV-1 mutant strains and WT HIV-1 RT.

Compd.	EC ₅₀ (μmol/L) ^a							IC ₅₀ (μmol/L) ^b
	L100I	K103N	Y181C	Y188L	E138K	F227L+V106A	K103N+Y181C	
B1	0.021 ± 0.015	0.016 ± 0.0071	0.047 ± 0.019	0.083 ± 0.015	0.038 ± 0.014	34.30 ± 4.12	0.074 ± 0.03	0.10 ± 0.017
B2	0.016 ± 0.0043	0.018 ± 0.0048	0.083 ± 0.015	0.45 ± 0.059	0.031 ± 0.016	30.84 ± 5.86	0.289 ± 0.15	0.045 ± 0.0058
B3	0.072 ± 0.0082	0.040 ± 0.016	0.14 ± 0.060	0.99 ± 0.28	0.052 ± 0.0096	>35	0.91 ± 0.25	0.077 ± 0.012
2	5.30 ± 1.49	7.78 ± 1.97	5.54 ± 1.45	104.24 ± 81.14	4.51 ± 0.37	>35	114.62 ± 58.88	3.21 ± 0.80
DOR	0.0066 ± 0.0017	0.042 ± 0.0013	0.025 ± 0.0023	0.50 ± 0.15	0.0075 ± 0.0026	17.35 ± 6.99	0.142 ± 0.0569	0.044 ± 0.005

^a EC₅₀: The effective concentration required to protect MT-4 cells against viral cytopathicity by 50%, and values were averaged from at least three independent experiments.

^b IC₅₀: Inhibitory concentration of test compounds required to inhibit WT HIV-1 RT activity by 50%. The data were obtained from the same laboratory (Prof. Erik De Clercq, Rega Institute for Medical Research, KU Leuven, Belgium) with the same method.

of **C7** and **C8** with methyl group achieved no positive effect (**C10** and **C11**).

The promising potency of compounds **B1–B3** encouraged us to further evaluate their inhibitory activity against a panel of clinically observed single and double mutants (L100I, K103N, Y181C, Y188L, E138K, F227L+V106A, and K103N+Y181C), and the results were summarized in Table 3. **B1–B3** had low nanomolar activity toward the tested HIV-1 mutant strains except for F227L+V106A. The most potent compound **B1** possessed almost comparable inhibitory activity to DOR toward L100I, K103N, Y181C, Y188L, E138K, F227L+V106A, and K103N+Y181C. Notably, **B1** was three- and six-fold more active than DOR against K103N and Y188L, respectively. A two-fold increase in the potency of **B1** against K103N+Y181C was observed compared to DOR.

The inhibitory activity of **B1–B3** against WT HIV-1 reverse transcriptase was also assessed. The results were illustrated in Table 3. Compounds **B1–B3** possessed nanomolar inhibitory activity toward WT HIV-1 reverse transcriptase, which was almost equivalent to DOR (IC₅₀ = 44 nmol/L).

To characterize the binding mode of **B1** within the non-nucleoside binding pocket of WT reverse transcriptase, molecular docking was carried out using the docking program Glide, and the protocol used was Induced Fit Docking. The structure of HIV-1 reverse transcriptase (RT) was downloaded from the PDB database (PDB code: 4NCG). The docking results were visualized by PyMOL. As shown in Figs. 2A and I, **B1** was well positioned into the non-nucleoside reverse transcriptase inhibitors binding pocket and showed a similar binding conformation to that of DOR. The biphenyl fragment was inserted into the hydrophobic aromatic tunnel formed by Y181, Y188, F227 and W229, exhibiting positive π - π stacking interactions with W229, Y188 and F227, respectively. Two important hydrogen-bonding interactions between the triazolone moiety and amide K103 (C-N...H-N distance = 2.2 Å; H...O=C distance = 1.7 Å) were observed. Besides, **B1** fitted well into the pockets of the L100I, K103N, Y181C, Y188L, E138K and K103N+Y181C mutants, respectively, and several common features (hydrogen bonds, and hydrophobic and electrostatic interactions) were still maintained as those in the WT RT en-

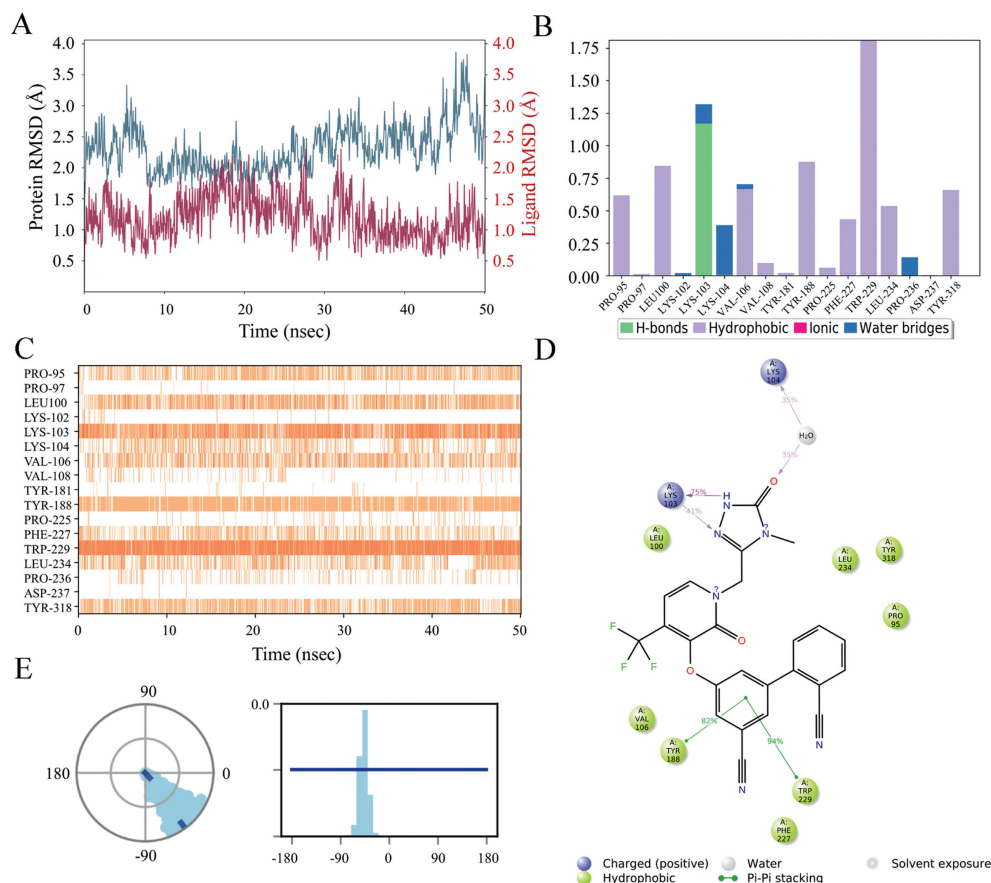


Fig. 3. Molecular dynamics simulations analysis of compound **B1** with WT HIV-1 reverse transcriptase (PDB code: 4NCG); (A) RMSD of compound **B1**; (B, C) Protein-ligand contacts analysis of MD trajectory; (D) Two-dimensional (2D) interaction diagram and interactions that occurred more than 30.0% of the simulation time in the selected trajectory; (E) The conformation of the torsion throughout the simulation (dial plot) and the probability density of the torsion (bar plot).

zyme (Figs. 2B–F and H). However, compound **B1** adopted a fully flipped conformation in the binding pocket of F227L+V106A mutant strain (Fig. 2G), resulting in reduced potency due to the loss of the key hydrogen-bonding interactions with the K103 amide (C–N...H–N).

To gain further insight into the theoretical binding mode and docking complex stability of the best NNRTI inhibitors in this series, **B1** was simulated for 50 ns using the software Schrödinger Maestro 11.4 (PDB code: 4NCG) with default settings to simulate its binding to WT HIV-1 reverse transcriptase. As shown in Fig. 3A, the root-mean-square deviation (RMSD) fluctuations of **B1** were always smaller than that of the protein within 50 ns, indicating that the ligand **B1** remained at its original binding site throughout the entire process. The 4NCG-**B1** complex stabilized rapidly with the RMSD fluctuations below the allowable limit of 3 Å. Detailed schematic interactions of ligand **B1** with the protein residues over 50 ns were presented in Figs. 3B–D. Four kinds of interactions, including hydrogen bonds, hydrophobic, ionic, and water bridges, were involved in the whole process of molecular dynamics simulation (Fig. 3B). 0.7 represents that the specific interaction spans 70% of 50 ns (Fig. 3B) and when multiple contacts between protein and ligand are possibly observed with values exceeding 1.0. A darker orange shade represents more than one specific contact of some residues with the ligand (Fig. 3C). Molecular dynamics simulations showed that **B1** interacted with W229 via π - π stacking interactions for almost the entire 50 ns simulation time (Fig. 3C) and similar interactions between **B1** and Y188 were also observed. The triazolone of **B1** formed hydrogen bonds with K103 directly and a water-bridge hydrogen bond with K104. These interactions were

almost consistent with the docking results in Fig. 3A. The *ortho*-substituted CN group expanded the dihedral angle of the biphenyl ring (Fig. 3E), which was favorable for maintaining a suitable conformation in the binding pocket.

In summary, 31 new biphenyl-pyridone derivatives were synthesized and evaluated for their anti-HIV activity to enrich their structure-activity relationships. From this series prepared, compounds **B1–B3** with different *meta*-substituted biphenyl groups had low nanomolar activity against wild-type HIV-1 and clinically observed single/double mutant strains. Of these, the most active compound **B1** was comparable to doravirine ($EC_{50} = 17$ nmol/L) against WT HIV-1, which was 231-fold more potent than **2** ($EC_{50} = 3.93$ μ mol/L). Pleasingly, the cytotoxicity of **B1** against MT-4 cells was significantly reduced ($CC_{50} = 100$ μ mol/L) with a much higher SI value of 5923, compared with **2** ($CC_{50} = 28.24$ μ mol/L, SI = 8.60). Besides, the compound **B1** displayed nanomolar inhibitory activity against six clinically observed mutant strains (L100I, K103N, E138K, Y181C, Y188L and K103N+Y181C), and three of them, including K103N, Y181C and K103N+Y181C, were more sensitive to **B1** than both **2** and doravirine. Furthermore, **B1** possessed remarkably enhanced binding affinity to wild-type HIV-1 reverse transcriptase ($IC_{50} = 100$ nmol/L) compared to **2** ($IC_{50} = 3.21$ μ mol/L). Molecular docking study revealed that introducing an *ortho*-substituted cyano group on the phenyl ring enlarged its dihedral angle, which facilitated the localization of biphenyl fragment to the aromatic-rich region in a more suitable manner and contributed to enhancing their biological activity via π - π stacking interactions with W229, Y188 and F227. Furthermore, two crucial hydrogen-bonding interactions of the triazolone moiety with residue K103 were retained.

Also, molecular dynamic simulations demonstrated the stability of the protein-ligand complex throughout 50 ns. The discovery of **B1** represented a promising starting point in the development of even more efficacious anti-HIV drugs.

Declaration of competing interest

The authors declare that they have no known competing financial interests or personal relationships that could have appeared to influence the work reported in this paper.

Acknowledgments

This work was funded by the National Natural Science Foundation of China (No. 22077018). We also thank Fudan University for providing the sources of molecular modeling.

Supplementary materials

Supplementary material associated with this article can be found, in the online version, at doi:10.1016/j.ccllet.2023.108261.

References

- [1] E. De Clercq, Nat. Rev. Drug Discov. 6 (2007) 1001–1018.
- [2] A.S. Fauci, H.C. Lane, N. Engl. J. Med. 383 (2020) 1–4.
- [3] <https://www.unaids.org/en> (The latest data on HIV released by UNAIDS in 2022).
- [4] C. Beyrer, A. Pozniak, N. Engl. J. Med. 377 (2017) 1605–1607.
- [5] H. Jonckheere, J. Anné, E. De Clercq, Med. Res. Rev. 20 (2000) 129–154.
- [6] G.D. Li, Y. Wang, E. De Clercq, Acta Pharm. Sin. B 12 (2022) 1567–1590.
- [7] X. Zhang, Acta Pharm. Sin. B 8 (2018) 131–136.
- [8] S. Xu, L. Sun, W.A. Zalloum, et al., Chin. Chem. Lett. 34 (2023) 107611.
- [9] Y. Mehellou, E. De Clercq, J. Med. Chem. 53 (2010) 521–538.
- [10] R.J. Shattock, M. Warren, S. McCormack, C.A. Hankins, Science 333 (2011) 42–43.
- [11] E. De Clercq, J. Med. Chem. 62 (2019) 7322–7339.
- [12] D. Feng, F. Wei, Y. Sun, P.P. Sharma, T. Zhang, et al., Chin. Chem. Lett. 32 (2021) 4053–4057.
- [13] Z. Wang, S. Cherukupalli, M. Xie, W. Wang, X. Jiang, et al., J. Med. Chem. 65 (2022) 3729–3757.
- [14] C. Zhuang, C. Pannecouque, E. De Clercq, F. Chen, Acta Pharm. Sin. B 10 (2020) 961–978.
- [15] L.M. Zhao, S. Wang, C. Pannecouque, et al., Eur. J. Med. Chem. 240 (2022) 114581.
- [16] D. Li, C. Zhang, W. Ding, S. Huang, L. Yu, et al., Chin. Chem. Lett. 32 (2021) 1020–1024.
- [17] Q. Hao, X. Ling, C. Pannecouque, E. De Clercq, F. Chen, Chin. Chem. Lett. 34 (2023) 107663.
- [18] K. Jin, M. Liu, C. Zhuang, et al., Acta Pharm. Sin. B 10 (2020) 344–357.
- [19] R.L. Zhou, Z. Ju, C. Pannecouque, et al., Eur. J. Med. Chem. 246 (2023) 114939.
- [20] X. Ling, Q.Q. Hao, W.J. Huang, et al., Eur. J. Med. Chem. 247 (2023) 115042.
- [21] W. Ming, W.L. Lu, C. Pannecouque, et al., Eur. J. Med. Chem. 248 (2023) 115114.
- [22] Q. Deng, Q. Zheng, B. Zuo, T. Tu, Green Synth. Catal. 1 (2020) 75–78.